

## Electronic Supplementary Information

# Low-Cost and Facile One-Pot Synthesis of Singlecrystalline Nanostructured $\epsilon$ -Cu<sub>0.95</sub>V<sub>2</sub>O<sub>5</sub> Nanoribbon: High-Capacity Cathode Material for Rechargeable Li-Ion Batteries

Wen Hu<sup>ab</sup>, Xin-bo Zhang<sup>\*a</sup>, Yong-liang Cheng<sup>ab</sup>, Yao-ming Wu<sup>a</sup>, and Li-min Wang<sup>\*a</sup>

<sup>a</sup>State Key Laboratory of Rare Earth Resource Utilization, Changchun Institute of Applied Chemistry, Chinese Academy of Sciences, Changchun 130022, Jilin, China

<sup>b</sup>Graduate School of the Chinese Academy of Sciences, Beijing 100039, China

\*To whom correspondence should be addressed. Tel/Fax: (+86)431-85262447; E-mail:

xbzhang@ciac.jl.cn; lmwang@ciac.jl.cn

## Experimental Section

Cupric nitrate trihydrate ( $\text{Cu}(\text{NO}_3)_2 \cdot 3\text{H}_2\text{O}$ , Beijing chemical works, AR), vanadium pentoxide ( $\text{V}_2\text{O}_5$ , Beijing chemical works, AR), acetophenone ( $\text{C}_8\text{H}_8\text{O}$ , Sinopharm chemical reagent Co, Ltd., AR), deionized water, absolute alcohol and acetylene black (Hong-xin chemical works), N-methyl-2-pyrrolidinone (NMP, Aladdin reagent, AR), PVDF (Dupont company, 99.9%), separator (polypropylene film, Celgard), electrolyte (1M  $\text{LiPF}_6$  in ethylene carbonate (EC)/dimethyl carbonate (DMC) with the weight ratio of 1:1, Zhangjiagang guotai-huarong new chemical materials Co., Ltd). All the chemicals were used as received.

Amounts of 0.087 g  $\text{Cu}(\text{NO}_3)_2 \cdot 3\text{H}_2\text{O}$  and 0.0436 g  $\text{V}_2\text{O}_5$  were dispersed into mixture of 24 mL deionizer water and 150  $\mu\text{L}$  acetophenone. After the mixture had been stirred and then ultrasonication for 10 min, the resulting mixture was transferred into 30 mL Teflon-linked stainless steel autoclave and maintained at 200 °C for 15 hours, then cooled to room temperature naturally. The obtained black solids were collected by centrifugation, washed by deionized water and ethanol, and then vacuum dried at 70 °C for 12 h.

To investigate the phase structures of the products, X-ray diffraction (XRD) patterns were recorded by a Bruker D8 Focus power X-ray diffractometer with  $\text{Cu K}\alpha$  radiation. Scanning electron microscope (SEM) was performed by a Hitachi S-4800 field emission scanning electron microscope, whereas EDS was done using a Bruker AXS microanalysis at an accelerating voltage of 20 kV. Samples for SEM were prepared by dispersing the as-prepared product in ethanol by sonicating for about 30

min, and then depositing the sample onto a silicon wafer, attached to a SEM brass stub. A Philips TF-F20 (200 kV) transmission electron microscope (TEM) with an energy-dispersive X-ray spectrometer was used to obtain SAED patterns and local compositional information and to study the phase microstructure. Samples for all of these TEM experiments were prepared by dispersing the samples in ethanol, sonicating for 30 min to ensure adequate dispersion of the nanostructures, and evaporating one drop of the solution onto a 300 mesh Cu grid, coated with a lacey carbon film. The oxidation states of the constituent elements were measured with X-ray photoelectron spectroscopy (XPS) using Thermo ESCALAB 250 system and the XPSPEAK software was used for the fitting of the XPS spectra. The final aqueous reaction solution after removal of the solid precipitates was injected into the SHIMADZU GC-2010 device for componential analysis.

The positive electrodes were fabricated by mixing 80 wt% active materials, 10 wt% acetylene black and 10 wt% PVDF binder in appropriate amount of NMP as solvent. Then the resulting paste was spread on an aluminum foil by automatic film coater (micrometer doctor blade, MTI). After the NMP solvent evaporation in a vacuum oven at 120 °C for 12 h, the electrodes were pressed and cut into disks. A CR2032 coin-type cell was assembled with lithium metal as the counter and reference electrode and polypropylene film as a separator. The cells were constructed and handled in an argon-filled glovebox. The charge-discharge measurements were carried out using the Land battery system (CT2001A) at a constant current density in a voltage range of 2-3.6 V versus Li/Li<sup>+</sup>. The cells discharged/charged to different

voltages and maintained at that voltage for 3 h were opened in the glovebox, and the positive electrodes were washed with DMC and dried in the vacuum oven at 90 °C for 12 h. Then the working electrodes were analyzed by XRD and XPS, and the materials scratched off the electrodes were analyzed by SEM-EDX.

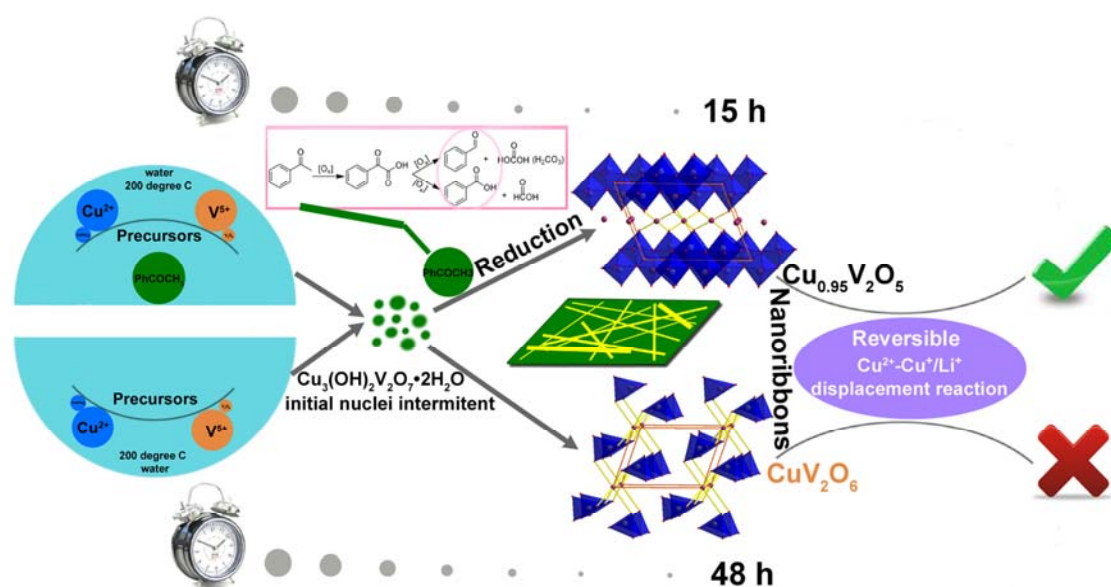


**Fig. S1** Different reaction pathways owing to acetophenone addition.

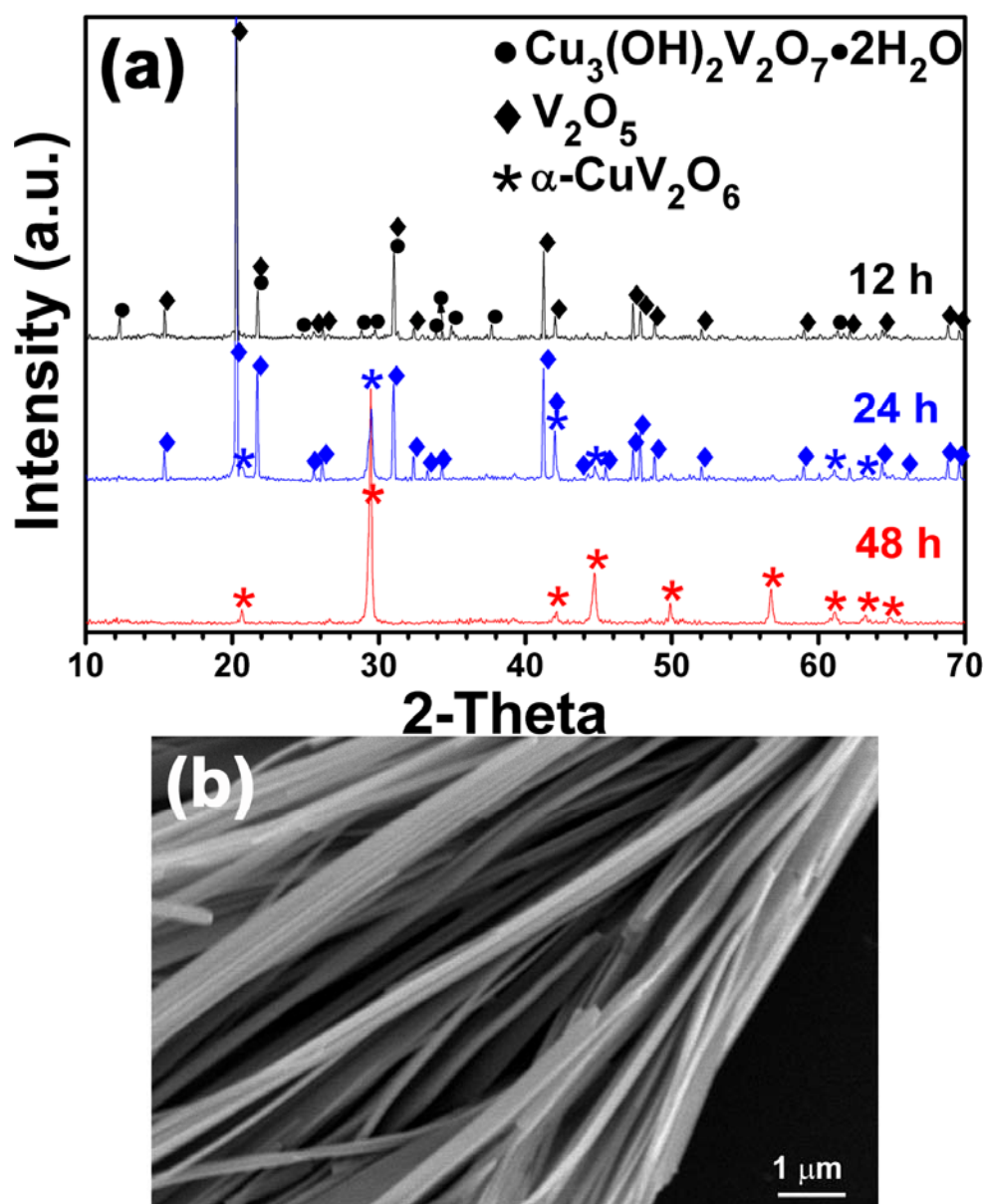


**Fig. S2** (a) XRD patterns of the final products prepared by the hydrothermal reaction of  $\text{Cu}(\text{NO}_3)_2 \cdot 3\text{H}_2\text{O}$  and  $\text{V}_2\text{O}_5$  at  $200^\circ\text{C}$  for different dwell times. The phase evolution process of  $\alpha\text{-CuV}_2\text{O}_6$  undergoes the same hydrated volborthite  $\text{Cu}_3(\text{OH})_2\text{V}_2\text{O}_7 \cdot 2\text{H}_2\text{O}$  crystalline intermediate to that of  $\epsilon\text{-Cu}_{0.95}\text{V}_2\text{O}_5$ . (b) SEM image of the as-synthesized  $\alpha\text{-CuV}_2\text{O}_6$  nanoribbons.

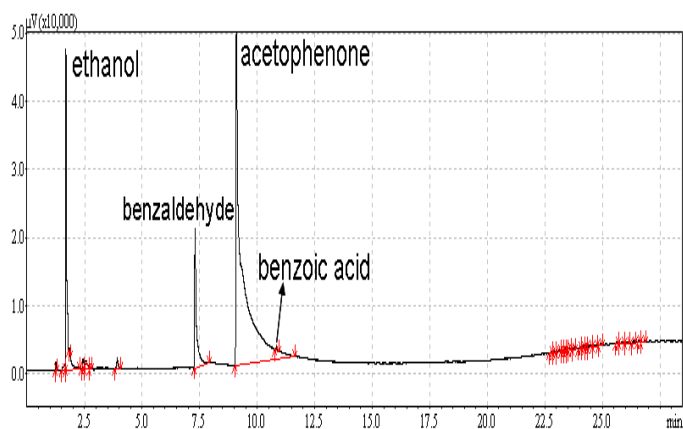


**Fig. S3** Gas chromatogram of the obtained reaction solution after particle removal.

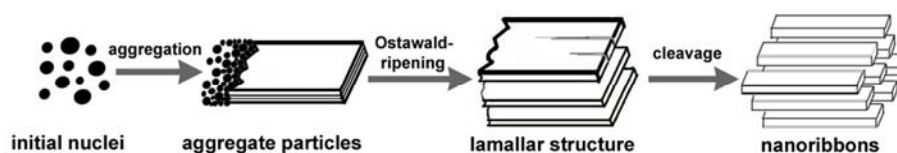


**Fig. S4** Schematic illustration of nanowires evolution in the synthesis of  $\epsilon\text{-Cu}_{0.95}\text{V}_2\text{O}_5$ .

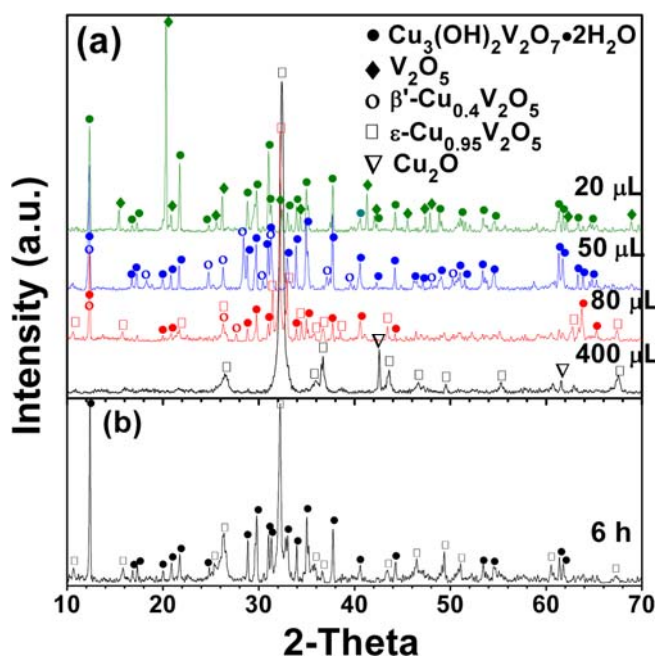


**Fig. S5** XRD patterns of the hydrothermal final products prepared under different amounts of acetophenone addition (a), and (b) during the course of reaction of 6 hours.

The XRD patterns (Figure S5a) show that the amount of acetophenone addition in hydrothermal reaction system is the key factor to determine whether  $\epsilon$ - $\text{Cu}_{0.95}\text{V}_2\text{O}_5$  with high purity can be obtained. When 20  $\mu\text{L}$  acetophenone is added to the autoclave, the final product is a mixture of  $\text{Cu}_3(\text{OH})_2\text{V}_2\text{O}_7 \cdot 2\text{H}_2\text{O}$  (PDF #46-1443) and  $\text{V}_2\text{O}_5$  (PDF #41-1426). As the amount of acetophenone is increased to 50  $\mu\text{L}$ ,  $\beta'$ - $\text{Cu}_{0.4}\text{V}_2\text{O}_5$  (PDF #46-0361) is formed together with the aforementioned  $\text{Cu}_3(\text{OH})_2\text{V}_2\text{O}_7 \cdot 2\text{H}_2\text{O}$ . When 80  $\mu\text{L}$  acetophenone is used, the first appearance of  $\epsilon$ - $\text{Cu}_{0.95}\text{V}_2\text{O}_5$  (PDF #18-0463) replaces most of the  $\beta'$ - $\text{Cu}_{0.4}\text{V}_2\text{O}_5$  phase and the peak intensity of  $\text{Cu}_3(\text{OH})_2\text{V}_2\text{O}_7 \cdot 2\text{H}_2\text{O}$  is decreased. If the amount of acetophenone is in the range of 120-200  $\mu\text{L}$ , highly pure  $\epsilon$ - $\text{Cu}_{0.95}\text{V}_2\text{O}_5$  will be obtained (Figure 1a in main text). However, when the amount of acetophenone exceeds the upper limit of the selected range, 400  $\mu\text{L}$  for example,  $\text{Cu}_2\text{O}$  impurity will mingle in the final product. As regards the dwell time for the hydrothermal reactions, 15 hours will be enough to get pure  $\epsilon$ - $\text{Cu}_{0.95}\text{V}_2\text{O}_5$  phase (Figure 1a in main text), or else,  $\text{Cu}_3(\text{OH})_2\text{V}_2\text{O}_7 \cdot 2\text{H}_2\text{O}$  can not be fully exhausted (Figure S5b).

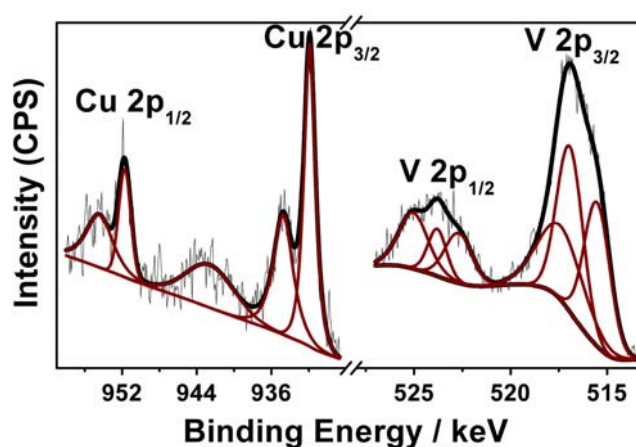


**Fig. S6** XPS spectra for copper 2p and vanadium 2p for  $\epsilon$ - $\text{Cu}_{0.95}\text{V}_2\text{O}_5$  nanoribbons.

In the Cu region, both of the peaks for Cu 2p<sub>3/2</sub> and 2p<sub>1/2</sub> can be deconvoluted into two components. The five peaks located at binding energies (BEs) of 931.9, 934.7, 942.8, 951.7 and 954.4 eV can be assigned to Cu<sup>+</sup> 2p<sub>3/2</sub>, Cu<sup>2+</sup> 2p<sub>3/2</sub>, the satellite peak of Cu<sup>2+</sup> 2p<sub>3/2</sub>, Cu<sup>+</sup> 2p<sub>1/2</sub> and Cu<sup>2+</sup> 2p<sub>1/2</sub>, respectively. The V 2p region shows broadening, peak multiplicity evidencing several distinct valences of vanadium species in the ε-Cu<sub>0.95</sub>V<sub>2</sub>O<sub>5</sub> nanoribbons. The six deconvoluted peaks at the BEs of 515.5, 516.9, 517.3, 522.7, 523.8 and 525 eV correspond to V<sup>3+</sup> 2p<sub>3/2</sub>, V<sup>4+</sup> 2p<sub>3/2</sub>, V<sup>5+</sup> 2p<sub>3/2</sub>, V<sup>3+</sup> 2p<sub>1/2</sub>, V<sup>4+</sup> 2p<sub>1/2</sub> and V<sup>5+</sup> 2p<sub>1/2</sub>, respectively. From the spectra we have found that both Cu and V are mixed-valent between Cu<sup>+</sup> and Cu<sup>2+</sup> and between V<sup>3+</sup>, V<sup>4+</sup> and V<sup>5+</sup>, respectively.

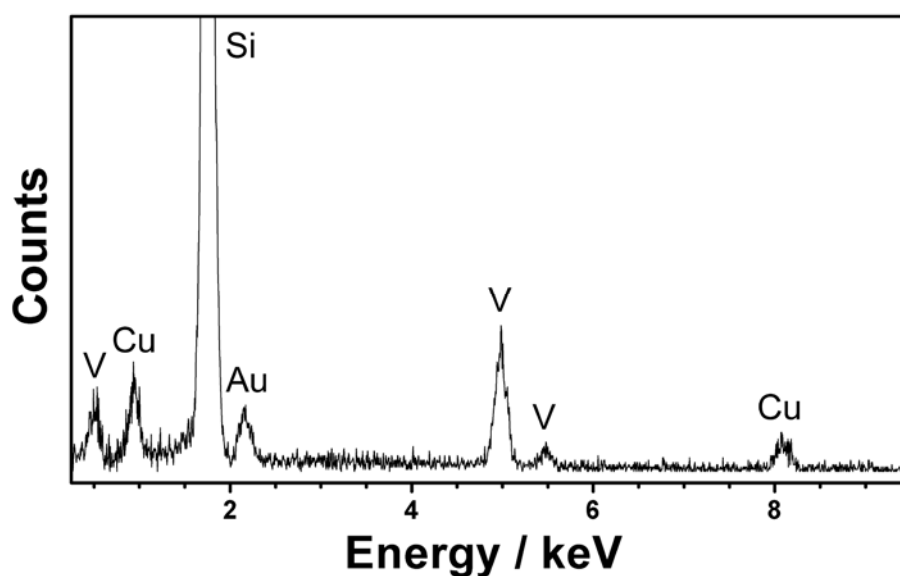


**Fig. S7** EDS spectrum of the as-synthesized ε-Cu<sub>0.95</sub>V<sub>2</sub>O<sub>5</sub> nanoribbons. The presence of Si is due to the usage of singlecrystal silicon wafer for SEM. The signal of Au originates from an ultrathin gold coating as electrically conducting material deposited on the specimens.

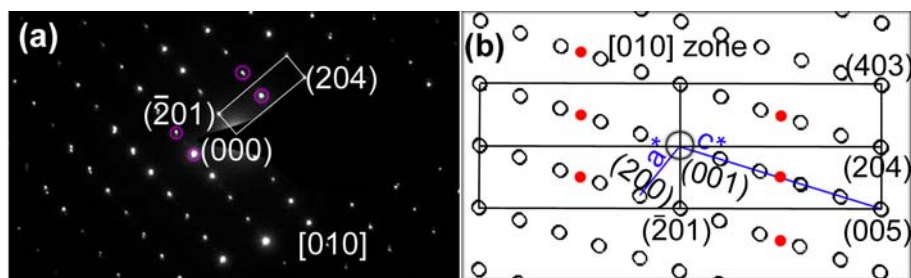


**Fig. S8** (a) [010] zone SAED pattern, (b) computer-generated reciprocal lattice pattern taken along the [010] zone axis. The regular appearance of some forbidden spots is marked with small red circles.

Inset of Figure 1c presents a very interesting [010] SAED pattern from the  $\epsilon$ -Cu<sub>0.95</sub>V<sub>2</sub>O<sub>5</sub> nanoribbons. Here we provide two possible explanations to interpret it. Presumption 1: the reciprocal lattice is comprised of two suits of completely identical diffraction spots. The configuration of the valid Bravais lattice is a simple rectangle. One would be puzzled because each rectangle seems to have a center. In fact, the plausible centered spots in every rectangle weave the other similar suit of simple rectangles, represented by one whose four vertexes have been marked by small open circles in the figure. Presumption 2: The valid Bravais lattice is a body-centered rectangle, implying a superlattice structure with c-doubling (Figure S8b). To be honest, we would like to believe the latter explanation. If the depiction of Presumption 1 is the fact, the stacking fault effect due to the lamellar nature of the ultrathin ribbon or two very small crystalline grains covered in the diameter of one electron beam do exist. It means the two counterparts (i.e. two layers or two grains) must be perfectly same, and what is more important is the justified orientation between the two. Considering the rigorous request for the two counterparts to fulfill

the Presumption 1, we think that the odds to get three similar SAED results in different conditions are astronomical. Therefore, it is reasonable to support Presumption 2 on the basis of copper ordering in the Cu(2) sites, although the superstructure has not been reported before in  $\epsilon$ -Cu<sub>0.95</sub>V<sub>2</sub>O<sub>5</sub>. Whatever argument is tenable, this SAED pattern shown in Figure S6a is the [010] zone of the  $\epsilon$  phase.

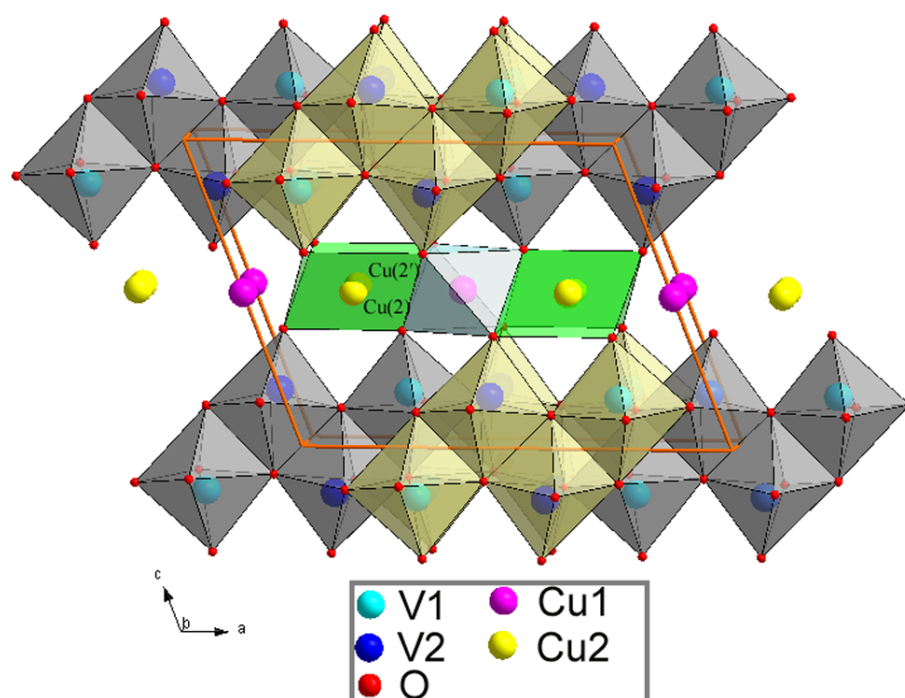


**Fig. S9** Crystal structure of  $\epsilon$ -Cu<sub>0.85-1</sub>V<sub>2</sub>O<sub>5</sub>.

Two independent vanadium atoms, V(1) and V(2), are located in distorted VO<sub>6</sub> octahedra having edges in common to form double zigzag ribbons (D4 layers as known) developed in the (001) plane and stacked along the [001] direction. The layers build up the (V<sub>2</sub>O<sub>5</sub>)<sub>n</sub> network, which incorporates two different oxygenated tunnels. Thus copper ions Cu(1) and Cu(2) take up two different crystallographic sites, corresponding to octahedral and square planar surroundings, respectively. Cu(1) sites

are almost fully occupied while for Cu(2) sites only half occupancy due to the short distance 1.847(2) Å between Cu(2) and Cu(2').

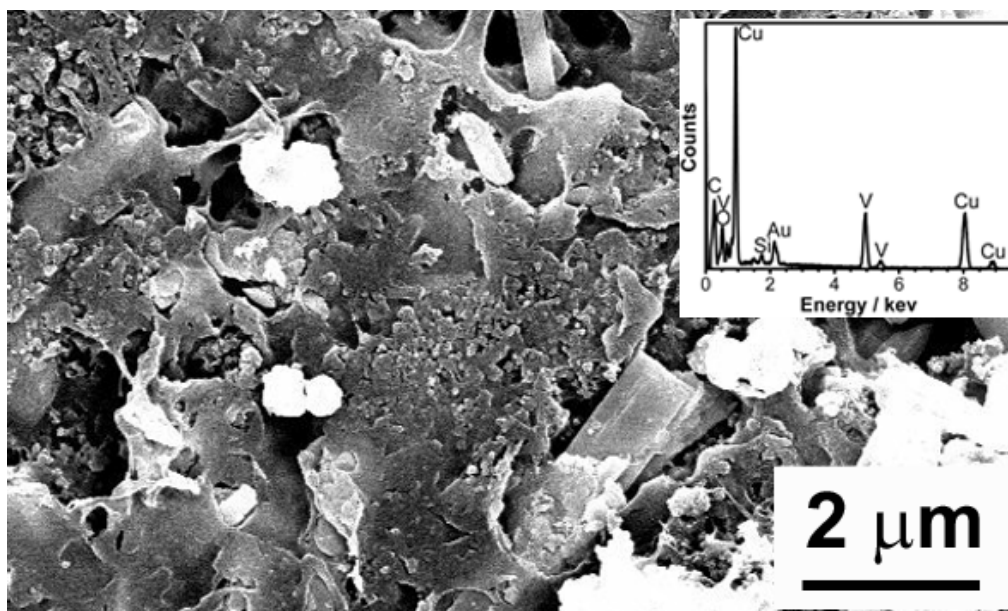


**Fig. S10** SEM-EDS results of electrode discharged to 2.72 V.